A Cell-Penetrant Manganese SOD-Mimic Is Able To Complement MnSOD and Exerts an Antiinflammatory Effect on Cellular and Animal Models of Inflammatory Bowel Diseases

Emilie Mathieu, Anne-Sophie Bernard, Nicolas Delsuc, Elodie Quévrain, Géraldine Gazzah, Barry Lai, Florian Chain, Philippe Langella, Maria Bachelet, Joelle Masliah, et al.

A cell penetrant manganese SOD-mimic is able to complement MnSOD and exerts an anti-inflammatory effect on cellular and animal models of inflammatory bowel diseases

Emilie Mathieu,[a,b]‡ Anne-Sophie Bernard,[a,b]‡ Nicolas Delsuc, [a,b] Elodie Quévrain,[a,b] Géraldine Gazzah,[a,b] Barry Lai,[c] Florian Chain,[d] Philippe Langella,[d] Maria Bachelet,[d] Joelle Masliah,[a] Philippe Seksik,[d] and Clotilde Policar* [a,b]

[a,b] Prof. Clotilde Policar*, Dr. Anne-Sophie Bernard, Emilie Mathieu, Dr. Nicolas Delsuc, Dr. Elodie Quévrain, Géraldine Gazzah; Département de Chimie, Ecole Normale Supérieure, PSL Research University — Sorbonne Universités, UPMC Univ Paris 06, Laboratoire des Biomolecules (LBM), 24, rue Lhomond, 75005 Paris, France E-mail: clotilde.policar@ens.fr
[c]Dr. Barry Lai; X-ray Science Division, Argonne National Laboratory, Argonne, Illinois 60439, United States.
[d]Dr. Florian Chain, Prof. Philippe Langella; INRA, Commensal and Probiotics-Host Interactions Laboratory UMR 1319 Micalis F-78350 Jouy en Josas, and AgroParisTech, UMR1319 Micalis F-78350 Jouy-en-Josas, France
[e]Prof. Philippe Seksik, Prof. Joelle Masliah, Dr. Maria Bachelet; Sorbonne Universites, UPMC Univ Paris 06, Ecole Normale Superieure, CNRS, INSERM, APHP, INRA, Laboratoire des Biomolecules (LBM), 27 rue de Chaligny, 75012 Paris, France

Correspondence to Prof. Clotilde Policar, Departement de Chimie, Ecole Normale Superieure, PSL Research University, UPMC Univ Paris 06, CNRS, Laboratoire des Biomolecules (LBM), 24 rue Lhomond, 75005 Paris, France France E-mail: clotilde.policar@ens.fr

‡ASB and EM contributed equally

Additional material available

Keywords: SOD mimics — anti-inflammatory agent — manganese complex — imaging — metal speciation —inorganic cellular chemistry

Supporting Information Placeholder

ABSTRACT: Inorganic complexes are increasingly used for biological and medicinal applications and the question of the cell-penetration and of the cell-distribution of metallodrugs is key to understand their biological activity. Oxidative stress is known to be involved in inflammation and in Inflammatory Bowel Diseases for which antioxidative defenses are weakened. We report here the study of a Mn-complex **Mn1** mimicking superoxide dismutase, a protein involved in the cell protection against oxidative stress, using an approach in *inorganic cellular chemistry* combining investigation of **Mn1** intracellular speciation using mass spectrometry, of its quantification and distribution using electron paramagnetic resonance and spatially-resolved X-ray fluorescence with evaluation of its biological activity. More precisely, we have looked for and find the MS-signature of **Mn1** in cell lysates and quantified the overall Mn-content. Intestinal epithelial cells activated by bacterial lipopolysaccharide were taken as a cellular model of oxidative stress and inflammation. **Mn1** exerts an intracellular anti-inflammatory activity, remains at least partially coordinated, with a diffuse distribution over the whole cell and functionally complements mitochondrial MnSOD.

INTRODUCTION

Exploring inorganic compounds in biological or cellular environments requires translating our knowledge from the round-bottom flasks to the cells. Cellular uptake, location inside cells, stability in intricate biological environments, are key features determining bio-activity that have to be studied.[1, 2] Here, we apply a general approach combining evaluations of the biological activity in a cellular model, with the exploration of the speciation, quantification of the intracellular content and cellular location in the case of the study of a Mn-complex mimicking the activity of the superoxide dismutase (SOD).[2] Correlating the intrinsic activity and the bio-activity in a cellular context, with the actual intracellular concentration, distribution and speciation, is important to decipher the relevant parameters controlling the activity in a biological context. This is surely one of the bases for an inorganic cellular chemistry approach, also more generally called inorganic chemical biology.[1-3] Bio-activities are usually reported against incubation concentrations, but they should also be analyzed as a function of the actual intracellular parameters.[4] Indeed, an intrinsic activity may remain silent if the compound does not enter the cell, or can be finely modulated by the concentration and also by the location inside cells.[5] This is why we clearly need to go beyond the mere observation of macroscopic effects on cell-cultures or biological tissues. To that extent, intracellular quantification and imaging —at the single cell level or within tissues substructures— are key experiments to provide a full understanding of bio-activity.[6]

Superoxide dismutases (SODs) are metalloenzymes that catalyse the dismutation of superoxide ($O_2^{\cdot-}$), a byproduct of respiratory metabolism in living aerobic systems. These proteins are part of the cellular antioxidant protection controlling reactive oxygen species (ROS), including superoxide. Oxidative stress is observed when the balance between ROS production and protective pathways is broken and occurs in a wide range of pathophysiological disorders — aging, neuro-degenerative diseases, chronic inflammation, etc.[7] Oxidative stress and inflammatory bowel diseases

(IBD) have been linked, oxidative stress being thought to sustain and amplify the inflammation in a vicious circle.[8-10] Moreover, a weakening of the anti-oxidant defenses regulating the flow of ROS has been observed in IBD:[11] in epithelial cells from patients with IBD, the mitochondrial manganese SOD (MnSOD) is over-expressed but in an enzymatically inactive form and the cytosolic copper SOD (CuSOD) content decreases with inflammation.[12] Convergent data support anti-oxidant therapies for IBD management.[8, 13-16] For instance, 5-aminosalicylic acid (5-ASA), currently used as the first therapeutic line in ulcerative colitis, is thought to act in part via its anti-oxidant effect,[11, 17, 18] and purified CuSOD has been efficiently tested in murine colitis models.[19] However, the use of proteins for therapeutics is generally associated with major drawbacks, including low cellular penetration, short half-life, and immunogenicity.[20] These shortcomings can be overcome by using low molecular weight redox active complexes mimicking SOD activity.[21-25] Manganese complexes are particularly valuable in this context since manganese ion is known to be less toxic than copper and iron ions,[7, 26] the other cations encountered at the active site of SODs but which can be a source of additional oxidative stress if released. Indeed, to date, a large variety of Mn-derivatives have been reported for their ability to react with superoxide and mimick SOD activity:[21, 23, 24, 27] free Mn^{II} [28, 29] but also Mn coordinated to salen derivatives,[30-32] cyclic polyamines,[20, 33-38] tri- or dipode N-centered ligands,[39-46], 1,2-ethanediamine centered ligands,[47-49] desferrioxamine derivatives[33, 50, 51] polyaminocarboxylato[52-54] or polycarboxylato ligands,[55] peptides,[56-58] as well as Mn^{III}-porphyrins,[59-64] phtalocyanines,[65] or biliverdine Mn-dinuclear complexes.[66] *In vivo* models have shown unambiguously the beneficial effect of these SOD mimics for the protection against radiation injuries,[67-70] and improvement of the therapeutic index in chemotherapia,[71] protection against chemical stress,[71, 72] ischemia reperfusion injury,[73-76] neuronal oxidative stress,[77, 78] endotoxic shock,[79] diabete,[80] or inflammation.[81] SOD-mimics have proven their efficiency to rescue SOD deficient cells,[66, 80, 82-84] cells under irradiation,[85-87] or chemical stress or infection,[71, 72] and in cells activated for ROS production such as macrophages[88, 89] or human leukemia cells.[65] SOD mimics represent also an appealing and promising approach in the field of IBD.[15, 16] Complex **Mn1** is a manganese SODm (Fig. 1A), bio-inspired from the active site of MnSOD and reproducing the coordination sphere of the metal center of this metalloenzyme,[23] that was previously described by our group. We reported its good intrinsic catalytic anti-superoxide activity which is associated with a cycling between two redox states Mn^{III}/Mn^{II},[90] as well as its intracellular anti-superoxide effect in activated murine macrophages demonstrating its ability to efficiently reduce the superoxide flow in this cellular model.[89] We aim to go further and investigate the potential role of the SOD mimic **Mn1** in controlling gut inflammation. For this purpose, we have used an intestinal epithelial cell line able to activate inflammation pathways after lipopolysaccharide (LPS) challenge, known to induce oxidative stress,[8, 13, 14, 91, 92] developed in our laboratory and labelled HT29-MD2. Briefly, HT29-MD2 is a HT29 intestinal epithelial cell-line stably transfected to over-express the protein MD2 conferring sensitivity to LPS, which is associated with an inflammatory response.[93, 94]

In the following, we combine in an inorganic cellular chemistry approach, characterization of **Mn1** — including metal-ligand stability constants, stability in growth medium, quantification of the intracellular content upon incubation, characterization in cell-lysates by mass spectrometry and imaging in cells using micro-X-fluorescence — with evaluations of the biological activity in cellular and animal models of IBD. We investigated the effect of **Mn1** on both the expression and activity of anti-oxidant protective enzymes (MnSOD and CuSOD) and inflammatory markers (IL8 and COX2). Additionally, an *in vivo* assay using a murine colitis model was set up to assess the efficiency of **Mn1**.

EXPERIMENTAL SECTION

Material

Information about chemicals is provided in the SI.

Preparation of the complexes

Complex **Mn1** (**Zn1**) was prepared by addition of 1 eq. of $MnCl_2$ ($ZnBr_2$) to a solution of $\mathbf{L}^{90}$ in HEPES buffer (100 mM, pH 7.4) at 5 mM and then diluted in culture medium at the desired incubation concentration. See the structures in Fig. 1.

Isothermal Calorimetric titration (ITC)

Dissociation constant of the manganese complex was determined by recording the heat of complexation with a Nano Isothermal Titration Calorimeter from TA Instruments. In a typical experiment, a ligand **L** solution (500 µM) in HEPES buffer (pH 7.4, 100 mM) containing NaCl (150 mM) in the calorimetric cell was titrated by a $MnCl_2$ solution (5 mM) (25 injections of 10 µL every 300 s under stirring at 25°C). Dilution heat was obtained in a separate measurement by injection of $MnCl_2$ into the buffer and was subtracted from the titration experiment. Thermogramms were used to obtained a binding isotherm which was fitted by a one binding site L:M model using NanoAnalyze program provided by TA Instruments, to obtain the dissociation constant K_d (Fig. S1 A and B).

UV-vis and electrochemistry

Mn1 stability over time in culture medium was assessed by UV-visible spectroscopy and cyclic voltammetry. UV-visible spectra were recorded on a CARY-5 UV–vis spectrophotometer using a double beam mode with media as the reference. Spectra of **Mn1** (500 µM) in complete medium (DMEM, 10% FBS, 0.1% blasticidin). were recorded at 37 °C for 8 h in semi-micro quartz cuvette (0.2 cm path length). Cyclic voltammograms were recorded at 37 °C under argon atmosphere on an Autolab µAUTOLABIII/FRA2 (Metrohm) at 0.5 $V.s^{-1}$. The auxiliary electrode was a Pt wire and the working electrode was a glassy carbon disk carefully polished before each voltammogram (diameter 3 mm). The reference electrode was a

SCE electrode. Cyclic voltammogram of **Zn1** was also recorded (see Fig. S1C).

Cell culture

HT29-MD2 intestinal epithelial cells were used for all experiments. HT29 human colon adenocarcinoma were obtained from the European Collection of Cell Cultures (ECCC, Wiltshire, UK) and stably transfected to over-express MD2 as previously described.[93] Cells were cultured in DMEM supplemented with 10% of heat inactivated foetal bovine serum (FBS), 1% of penicillin-streptomycin and 0.1% of blasticidin (10 µg/mL) at 37 °C in a 5% CO_2/air atmosphere.

Intracellular quantification of Mn1 by EPR

Mn1 was quantified by determining Mn^{2+} total content in HT29-MD2 cells lysates using Electron Paramagnetic Resonance (EPR). Cells were cultured in a 75 cm^2 flask to reach 90% of confluency. They were incubated with media only, **Mn1** or $MnCl_2$ (100 µM) for 0.5 to 7 hours, at 37 °C. After a washing with NaCl 0.9%, a chaotropic shock was performed by adding a solution of NaCl 1 M. Cells were washed (EDTA 50 mM, 2 washings NaCl 0.9%). They were harvested by scraping and centrifuged at 4°C during 10 min at 900 rpm. Supernatant was removed, 100 µL of milliQ water was added and two freezing/thawing cycles in liquid nitrogen were performed. Protein content was determined for each sample (See SI). Cell lysates were acidified with $HClO_4$ 70 % (w/w). A calibration curve was established using $MnCl_2$ in water acidified with $HClO_4$ and the quantification of the Mn-content was performed using the two first lines in the six-line Mn^{II} X-band EPR-spectrum and reported *per* mg of proteins (Fig. 2). EPR spectra were recorded on a Elexsys 500 spectrometer from Bruker in a glass capillary tube: frequency: 9.82 GHz, microwave power: 32 mW, amplitude of the modulation: 2G, 9 scans, room temperature. The same procedure was used to determine Mn-content in mitochondria enriched-fractions (see SI and Fig. S2).

LC-MS/MS: Intracellular stability of Mn1

Intracellular stability of **Mn1** in cells was investigated using LC-MS/MS. LC-MS of pure compound **Mn1** (1 µM) in water showed two peaks corresponding to the free ligand and the expected complex (m/z 355.2 and 408.2 respectively), meaning that partial decoordination occurs under the LC-MS conditions. By MS-MS analysis, the ligand L and **Mn1** exhibited different fragmentation patterns (m/z 249.2, 167.2 and 302.2, 248.2 respectively) (Fig. S3), from which a clear identification of **Mn1** inside cells can be obtained. A lysate of cells incubated with **Mn1** (100 µM, 3 h) was prepared as explained for EPR experiments, without addition of perchloric acid. The lysate was diluted with a maximum volume of 0.5 mL of ultrapure water and filtered over membrane with a 3 kDa cutoff. The resulting filtrate and a solution of complex **Mn1** in water were analyzed by a QTRAP LC–MS/MS system Applied Biosystem (injection of 10 µL). The LC system consisted of a Dionex-LC Packings Ultimate Plus integrated micro-HPLC system. A Dionex Acclaim Pepmap100 column (150 mm Å~ 1 mm i.d., C18, 3 µm particle size, 100 Å pore size) was used for the separation, with a gradient of 0–60% B in 75 min (solvent A = water–acetonitrile, 98:2, v/v, with 0.1% formic acid, solvent, B = acetonitrile–water, 98:2,v/v, with 0.1% formic acid) and a flow rate of 10 µL min^{-1}. The column output was connected to an Applied Biosystems Qtrap LC–MS/MS system mass spectrometer through a NanoSpray ion-source inter- face (Spray voltage set to 2.4 kV, desolvating potential (DP) set to 40 V, collision energy (CE) set to 30 V). The LC–MS/MS system was controlled by Analyst 1.4.2 software (Applied Biosystems), allowing a 2.7 s cycle of 4 experiments for mass spectra acquisition: one full single MS by scanning the linear trap followed by three MS/MS experiments on the (pseudo-) molecular ions of the compounds. MS/MS optimization experiments on standard compounds were performed by direct injection on a 1 µL loop Rheodyne LC injection valve connected to a TurboIonspray source, at a 20 µL.min^{-1} flow rate of solvent A (Ionspray voltage set to 5.5 kV, DP = 40 V, CE = 30 V).

Synchrotron radiation X-ray fluorescence microscopy: Intracellular distribution of Mn1

The intracellular distribution of Mn in control cells and cells incubated with **Mn1** or $MnCl_2$ was determined using synchrotron radiation X-ray fluorescence microscopy. HT29-MD2 cells were seeded on silicon nitride windows (size: 1 mm x 1 mm, thickness: 500 nm) in 24-wells plate (75000 cells/well). After 36 h, cells were incubated with medium only (control), **Mn1** or $MnCl_2$ (100 µM) for 2 h. Cells were washed with NaCl 0.9% and a chaotropic shock was performed by adding a solution of NaCl (1 M). They were then washed once with EDTA (50 mM), and twice with NaCl 0.9%. Cells were cryofixed in liquid ethane and freeze-dried. Mappings of intracellular manganese (Mn), potassium (K), phosphate (P), and sulfur (S) (Fig. 3 and S4) were performed on 2-ID-D beamline of Advanced Photon Source synchrotron (Argonne National Laboratory, Chicago, USA). Cells were located using a phase-contrast optical microscope. All measurements were conducted at room temperature, under a He atmosphere using a 6.8 keV monochomatic X-ray incident beam focused to 0.2 µm diameter. The fluorescence signal was detected with an integration time of 2 s per pixel, with a 200 nm pixel size, at 90° to the incident beam using a Vortex EM single element silicon drift detector. Images analyses were performed by using MAPS software from APS. Due to the last washing of cells with NaCl 0.9 % before cryofixation and freeze-drying, some NaCl crystals were present on silicon nitride membranes. The strong signal of Cl was then subtracted from other element signals.

Cell assays

Cells were seeded in 12 or 24 well-plates at 100 000 cells/well to reach 90% confluence after 3 or 4 days. Cells were incubated with **Mn1** and controls for 1 h (**Zn1**, $MnCl_2$: 100 µM; bovine CuSOD 100 U/mL; 5-ASA: 10 mM, 1 mM, 100 µM). Then, LPS was added (0.1 µg/mL, 6 hours). Supernatants were collected, and stored at -20 °C

before ELISA and LDH assay. Cells were washed with NaCl 0.9%, lysed in PBS containing 1% triton X-100 and protease inhibitors cocktail. They were harvested by scraping, and stored at -20°C before western blot, SOD activity on gels, cytotoxicity and protein quantification experiments.

Cytotoxicity assay
Cytotoxicity of **Mn1** and controls, with and without LPS, was assessed using lactate dehydrogenase (LDH) release assay with a limit for non-cytotoxicity chosen at 10% (see SI).

Protein Assay
Protein concentrations were determined in cell lysates using BCA protein assay reagents and bovine serum albumin (BSA) as standard according to the manufacturer's instructions (see SI).

Cell activation with LPS and incubation with the agents to be tested
Cells were seeded in 12-well culture plates to reach 90% of confluency after 3 or 4 days. They were then incubated with the agents to be assayed (typically, depending on the experiment: complex **Mn1** (100 µM), its redox silent analogue (Zn^{II} complex shown in Fig. 1A) **Zn1** (100 µM), $MnCl_2$ (100 µM) or bovine CuSOD (100 U/mL)) for 1 h and further incubated with LPS (0.1 µg/mL) for 6 more hours. Cell culture supernatants were then collected and stored at -20 °C before ELISA and LDH assay. Cells were washed with 0.9 % NaCl, lysed in PBS containing 1% triton X-100 and protease inhibitors cocktail. They were harvested by scraping, sonicated and stored at -20°C for western blot, SOD activity on gels, cytotoxicity and protein quantification experiments.

SOD activity on gel
SOD activity was determined by using the nitroblue tetrazolium (NBT) method.[95] A loading buffer containing 50 % of glycerol and 1 % of bromophenol blue solution in TRIS buffer (0.5 M, pH 6.8) was added to cell lysates (1/1 mixture). A non-denatured 10 % acrylamide gel was used and pre-electrophoresis (40 mA, 1 h, 4°C) was performed as described.[95] 100 µg of proteins were then loaded on gel and subjected to electrophoresis under non-denaturing conditions (40 mA, 4 h, 4°C) (NATIVE-PAGE). Gel was soaked and shaked in a staining solution containing NBT (2.43 mM), TEMED (28 mM) and riboflavin (0.14 M) in PBS for 20 min at room temperature in the dark. After washing with water, the gel was placed under UV light. Under illumination, the gel became uniformly purple except at locations containing SOD. Illumination was stopped when maximum contrast between the clear and the purple zones was achieved.

IL8 quantification
Levels of IL8 produced by cells were determined in cell supernatants using a commercially available ELISA kit according to the instructions of the manufacturer. IL8 levels were normalized by the protein content determined in the corresponding cell lysates.

COX2 and SODs analysis
Western blot analysis was performed to examine expression of COX2, MnSOD and CuSOD versus actin in cell lysates. Laemmli buffer was added to cell lysates (1/10 mixture) and the solution was heated at 100 °C for 3 min. 25 µg of denatured proteins were then loaded on a 10% acrylamide gel and subjected to electrophoresis (150 V at room temperature for 1.5 h) (SDS-PAGE). Proteins were transferred onto a nitrocellulose membrane (30 V, overnight at room temperature). The membrane was cut at 55 and 35 kDa to be revealed by the three antibodies because of their different sensitivity. It was first incubated for 1 h at room temperature in a solution containing non-fat dry milk (5 %) and Tween-20 (0.5 %) in PBS. After washing, membrane was incubated for 1 h at room temperature with primary antibodies diluted to 1/500 in milk solution. After washing, membrane was incubated for 1 h at room temperature with horseradish-peroxidase-conjugated secondary antibodies diluted to 1/5000 in 0.5 % of Tween-20 in PBS. Protein bands were visualized by chemiluminescence using ECL reagents. Intensity bands analysis was performed using ImageJ Software.

***In vivo* experiment**
Male C57BL/6 mice (6-8 weeks old) were purchased from Janvier Labs (St Berthevin, France) and maintained at the animal care facilities of the National Institute of Agricultural Research (IERP, INRA, Jouy-en-Josas, France) under specific pathogen-free conditions. Mice were housed under standard conditions for 1 week before experimentation start (Light/Dark 12h/12h, 20-22°C, 45-55% humidity, wood shaving as bedding and cellulose sheets as enrichment). They also had free access to water and food (R/M-H, Ssniff, Soest, Germany). All procedures were approved by the French ministry of Research and recorded under the project number 3445-2016010615159974.
Colitis was induced by intrarectal injection of 150 mg/kg of 2,4-dinitrobenzenesulfonic acid (DNBS) solution (Sigma, Saint-Quentin Fallavier) in 30% ethanol (EtOH). Final volume for this injection was 50 µl. Mice also received daily, starting the day of the DNBS injection, 100 µl of Phosphate Buffer Saline (PBS) containing either $NaHCO_3$ 4.2% (m/V, pH 8), $NaHCO_3$ 4.2% + $MnCl_2$ (8 mM) or $NaHCO_3$ + **Mn1** (4 mM) by oral gavage.
Mice were sacrificed by cervical dislocation. The colon was removed and opened longitudinally to assess macroscopic damages. A score was given to each mouse. Briefly, the macroscopic criteria include macroscopic mucosal damage (such as hyperhemia, ulcers, thickening of the colon wall measured with an electronic ruler, the presence of adhesions between the colon and other intra-abdominal organs) and the consistency of fecal material as diarrhea indicator.

Statistical analysis
All data are shown as mean ± SEM and were tested for statistical significance using the Mann-Whitney test or

Student's t test. Differences were considered significant when $p < 0.05$.

RESULTS

Stability of Mn1 in solution

The stability of **Mn1** was characterized in HEPES buffer (0.1 M, pH 7.4) and in cell culture medium. The apparent dissociation constant (K_d) in HEPES buffer was found to be $0.76 \pm 0.12\ 10^{-6}$ M at pH 7.4, as measured by Isothermal Titration Calorimetry (ITC) (Fig. S1 A and B). The stability of **Mn1** in cell culture medium was studied using both its UV-visible signature and redox properties. The UV-vis and the redox signature were recorded for several hours, with no modification (see Fig. 1B and C). The redox potential of the Mn^{III}/Mn^{II} couple in complex **Mn1** is *ca.* 0.15 V/SCE, which is close to that found for metallic center in all SODs and is the optimal redox potential for superoxide dismutation (ca. 0.12 V/SCE or 0.36 V/NHE).[23, 46, 96, 97] As expected, the Zn^{II} complex (**Zn1**) was found redox inactive (see Fig. S1C).

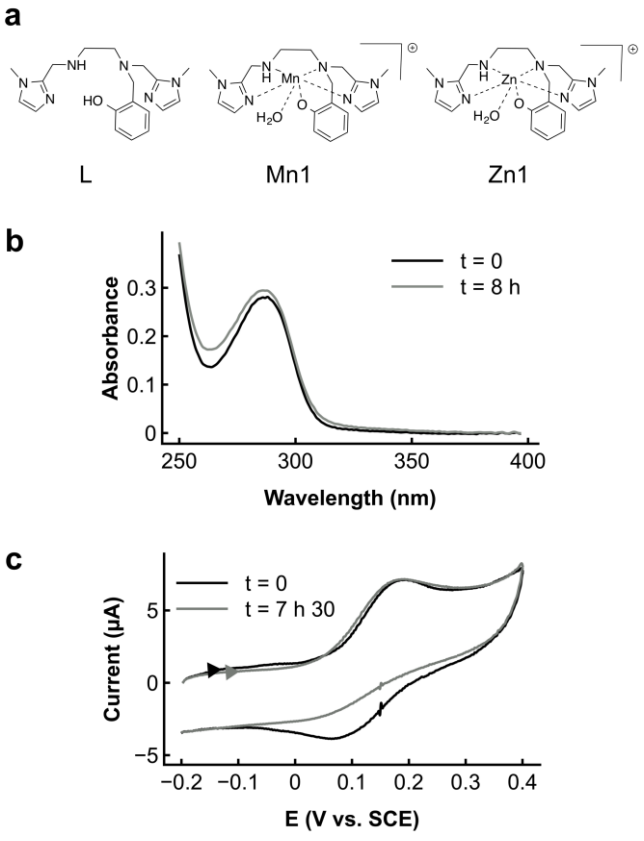

Figure 1: Structure of ligand L, Mn^{II}-complex Mn1, and Zn^{II}-complex Zn1 (a). Stability of Mn1 in solution (see also Fig. S1) Mn1 stability in cell culture medium was assessed by UV-visible spectroscopy (**b**) and cyclic voltammetry (CV, **c**), as the specific signature of the complex was observed after at least 7 hours. **b**: UV-visible spectra of **Mn1** recorded in complete media (DMEM, 10% FBS, 0.1% blasticidin) at 37 °C in a semi-micro quartz cuvette (l = 0.2 cm) using a double beam mode with media as a reference. **c**: Cyclic voltammogram of Mn1 in DMEM at 37 °C under argon atmosphere at a glassy carbon electrode, scan rate 0.5 $V.s^{-1}$. The forward peak corresponds to the Mn^{II} oxidation into Mn^{III} at Ep_a= 0.19 V/SCE. The fact that it does not decrease indicates that the complex is stable. The diminution of the current intensity of the return peak corresponds to the formation of an hydroxo-Mn complex in solution due to the increase in pH over time.[98]

Quantification and identification in cell-lysates

Electron paramagnetic resonance (EPR) can be used to quantify Mn^{2+}, which shows six-sharp lines in its hexa-aqua form. However, in conventional X-band EPR, the EPR spectrum of **Mn1** is broad because of the geometry of the Mn^{II} coordination sphere being distorted from the regular octahedron.[90] Hence, for quantification purpose, Mn^{2+} was released from the coordination with **L** by acidification of cell-lysates,[99] which had the additional advantage to favor the EPR responsive Mn^{II} redox state.

Total Mn^{2+} was titrated in acidified cell lysates using its six-sharp-line signature in X-band electron paramagnetic resonance (EPR) (Fig.2 and S2) and reported *per* mg of proteins (see protein assay in the SI). Note that this protocol frees manganese from all sites and leads to the evaluation of a total-Mn content.

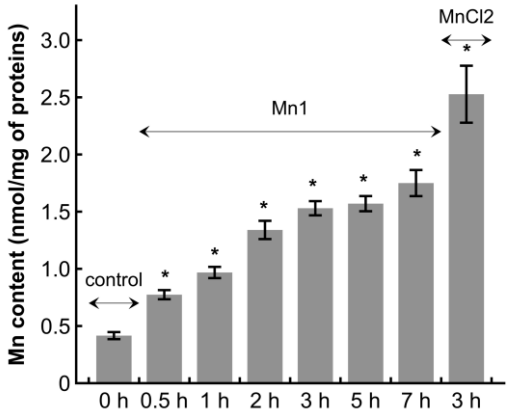

Figure 2: Titration of Mn^{II} in acid-digested lysates of cells HT29 MD2 by EPR. Cells were incubated at 37°C with **Mn1** (100 µM) from 0.5 to 7 h or with $MnCl_2$ (100 µM) for 3 h. Data represent means ± SEM for 5 independent experiments, * $p < 0.05$ versus control (see spectra in Fig. S2).

The cellular accumulation of **Mn1** upon incubation at 100 µM was observed with a stabilization of the cellular content after a 3h-incubation. The total Mn^{II}-content increased from 0.4 nmol/mg of proteins in the control cells to 1.75 nmol/mg of proteins after a 7h-incubation with **Mn1** at 100 µM. $MnCl_2$ (100 µM) showed a more efficient uptake.

The detection of a metal complex in biological environments is not straightforward, and LC-MS/MS is well-adapted for that purpose. **Mn1** exhibits a specific signature (see Fig. S3 A, B and C) that was clearly identified in cell-lysates (Fig. S3 D and E) using this method, showing **Mn1** was present in cells.

Cell distribution of Mn

Manganese was mapped on cryofixed freeze-dried cells using the highly spatially resolved synchrotron based X-fluorescence (resolution: 200 nm) with an excitation energy of 6.8 keV, which is above at the K-edge of Mn. The cellular manganese content in a single cell was higher after incubation with **Mn1** than in control cell and $MnCl_2$ was more efficiently uptaken (Fig. 3a), confirming EPR results. Mappings show a diffuse distribution of Mn, close to that of K (Fig. 3b) — known to be homogenously distributed in cells[100]—with higher amounts where the cell is the thickest. The distribution of other elements, such as P and S, are shown in Fig. S4.

To confirm the diffuse distribution in the overall cell, Mn was quantified using EPR in mitochondria-enriched cell fractions after 6h-incubation with $MnCl_2$ or **Mn1**, which shows that Mn is present in the mitochondria (see Fig. S2).

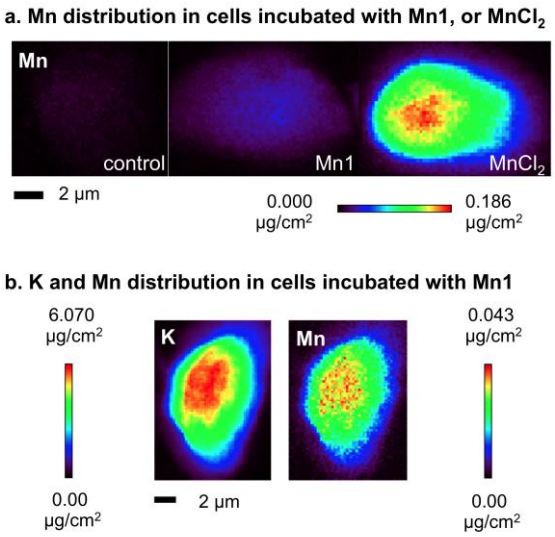

Figure 3: X-fluorescence mappings on cryo-fixed cells. a: Manganese detection by X fluorescence on cryofixed and freeze-dried cells HT29 MD2 incubated 2 h with medium only (control), **Mn1** (100 µM) or $MnCl_2$ (100 µM) shown with a single scale for the intensity to point at the difference in quantity. **b**: Potassium and manganese detection by X fluorescence on cryofixed and freeze-dried cell HT29 MD2 incubated with **Mn1** (100 µM). Images recorded on 2-ID-D beamline of APS synchrotron, excitation at 6.8 keV, integration time 2 s / pixel, pixel size 200 nm. Other maps (P and S) are given in Fig. S4.

Activity of Mn1 in HT29-MD2 epithelial cells

Cytotoxicity

Cytotoxicity was evaluated by LDH release assay. No cytotoxicity (LDH released <10%) was observed for **Mn1** at 100 µM or controls ($MnCl_2$, SOD, **Zn1**, $ZnBr_2$) in HT29-MD2 cells in steady state or after LPS challenge, whereas the non-coordinated ligand **L** was found cytotoxic in the same conditions and was then not further assayed. The Zn^{II}-complex (**Zn1**) constitutes a relevant control, as it is not able to catalyze the dismutation of superoxide but displays the same overall chemical structure and charge as **Mn1**, being thus its redox-silent analogue.

Anti-superoxide activity of Mn1 in HT29-MD2

Hydroethidine (HE) is a fluorescent probe used for detection of intracellular superoxide in cells.[101, 102] In HT29-MD2 steady state cells HE assay showed that **Mn1** was able to reduce oxidation of HE (Fig. S5), which was not the case for $MnCl_2$. This observation confirmed the intracellular anti-superoxide activity of **Mn1** as previously described by our group in macrophages.[89]

Effect of Mn1 on SODs expressions

Endogenous mitochondrial MnSOD and cytosolic CuSOD expression and activity were investigated in cell lysates by western blot and colorimetric assay on gel respectively, as shown on Fig. 4. As previously published on other cell lines,[8, 91] LPS challenge induced an over-expression of MnSOD, indicative of an oxidative stress mediated by LPS.[92] Very interestingly, **Mn1** was able to blunt the LPS-induced MnSOD up-regulation. In contrast, cytosolic CuSOD expression and activity were not significantly modified after LPS challenge, and incubation with **Mn1** induced only a weak, non-significant decrease (Fig. 4A). Neither $MnCl_2$ or purified SOD (Fig. 4), nor **Zn1** (Fig. S6) affected MnSOD over-expression after LPS challenge. In the absence of LPS, incubation of HT29-MD2 cells with **Mn1**, **Zn1** or $MnCl_2$ induced no significant modification of the expression of MnSOD or activity (Fig. S6).

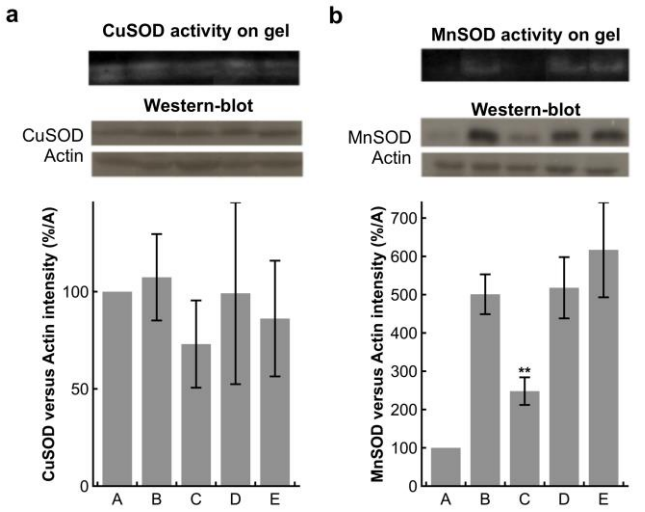

Figure 4: CuSOD (a) and MnSOD (b) expression and activity in intestinal epithelial cells activated with LPS. Representative experiment of CuSOD, and MnSOD expression and activity measured by western blot (WB) and colorimetric assay on gel respectively, after a 7 h incubation under several conditions: (A) control, (B) LPS, (C) **Mn1** (100 µM) + LPS, (D) $MnCl_2$ (100 µM) + LPS, (E) bovine CuSOD (100 U/mL) + LPS. LPS (0.1 µg/mL) was added after 1 h of incubation. *Top:* NBT assay on non-denatured gel for the measurement of the SODs activities, and WB to evaluate the expression of SODs in comparison with actin. *Bottom:* Quantification of MnSOD or CuSOD versus actin expression obtained by western blot analysis. Data represent means ± SEM for at least 4 (MnSOD) or 3 (CuSOD) independent experiments respectively, ** $p < 0.01$ versus B. Expression of MnSOD in controls without LPS and with LPS and HEPES are shown in Fig. S6. Full blots are shown in Figure S7.

*Anti-inflammatory activity of **Mn1***

The anti-inflammatory activity of the complex **Mn1** was evaluated by quantifying two markers of inflammation — the pro-inflammatory chemokine interleukine 8 (IL8) and cyclo-oxygenase 2 (COX2).[93] **Mn1** was shown to be more efficient against inflammation than 5-ASA, which is an anti-inflammatory agent currently used as the first therapeutic line in IBD[11] (see Fig. S10). LPS-induced IL8 as well as COX2 levels were significantly decreased in presence of **Mn1**, with *ca*. 65 % of inhibition for IL8 secretion (Fig. 5). Upon incubation with $MnCl_2$, or purified bovine CuSOD, no significant decrease of IL8 or COX2 was observed. Similarly, **Zn1**, the redox-inactive analogue of **Mn1**, did not decrease IL8 secretion (Fig. S11).

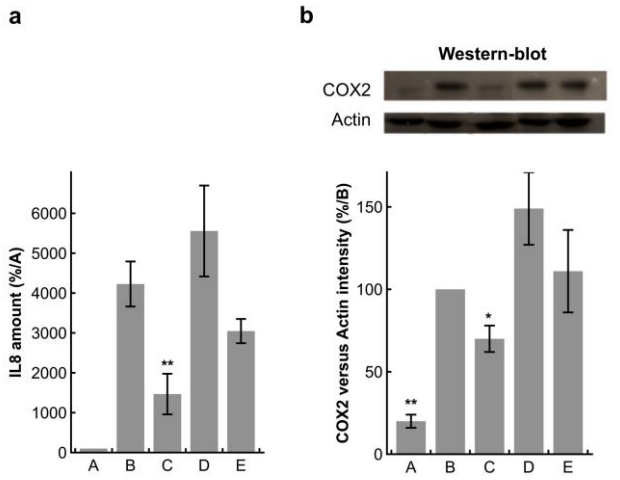

Figure 5: IL8 and COX2 expression in intestinal epithelial cells activated with LPS. Anti-inflammatory activity in HT29-MD2 cells after a 7 h incubation under several conditions: (A) control (B) LPS, (C) **Mn1** (100 µM) + LPS, (D) $MnCl_2$ (100 µM) + LPS, (E) bovine CuSOD (100 U/mL) + LPS. LPS (0.1 µg/mL) was added after 1 h of incubation. **a**: IL8 secretion was measured by ELISA in supernatants. Data represent means ± SEM for at least 5 independent experiments, ** $p < 0.01$ versus B. Controls without LPS and with LPS and HEPES are shown in Fig. S11. Note that, without LPS, no significant differences were observed between all these conditions (see Fig. S**11**, control, **Mn1**, $MnCl_2$, HEPES) or upon incubation with **Zn1. b**: representative experiment of COX2 and actin expression measured by western blot (top) in cell lysates and quantification of COX2 versus actin expression (bottom). Data represent means ± SEM for at least 4 independent experiments, * $p < 0.05$ and ** $p<0.01$ versus D. Full blots are shown in Figure S8.

Effect of SODm Mn1 in a chemically induced colitis in mice

In order to assess its anti-inflammatory effect *in vivo*, **Mn1** was administered by oral gavage in mice subjected to DNBS-induced colitis. No change in colon lengths was observed in the three groups (vehicle ($NaHCO_3$), $MnCl_2$, and **Mn1**, Fig. 6d). Macroscopic score of colitis in mice treated by **Mn1** was lower than in mice treated by vehicle or $MnCl_2$, but the difference was weak (Fig. 6b). In this model mortality was observed in the case for mice gavaged with vehicle or $MnCl_2$, with 2 deaths out of 8 mice in both cases. Interestingly, all mice survived with **Mn1**-gavage (Fig. 6a). **Mn1** was also able to reduce weight loss compared to vehicle and $MnCl_2$ (Fig. 6a and 6b). Moreover, mice treated by **Mn1** started to recover earlier than other mice.

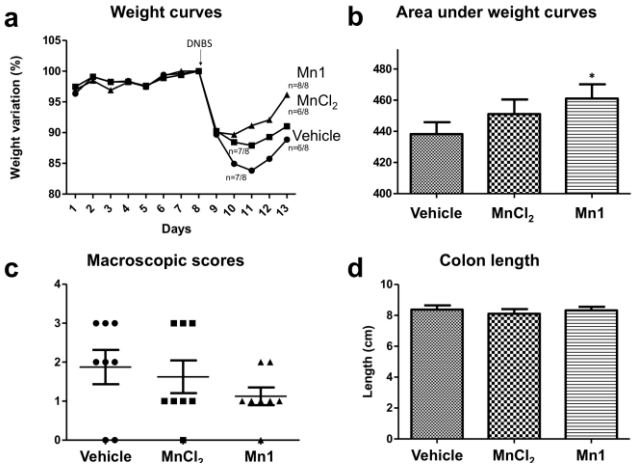

Figure 6: Effect of Mn1 in DNBS-induced colitis mice. **Mn1** anti-inflammatory effect was investigated in DNBS-induced murine model of colitis by looking at weight variation (**a**, **b**), macroscopic scores (**c**), and colon length (**d**). Colitis was induced by intrarectal injection of DNBS (150 mg/kg, 50 µL) in adult male C57BL/6 mice at day 8 after acclimatization start. Mice were treated daily by oral gavage, starting the day of DNBS injection, with 100 µL of vehicle ($NaHCO_3$ 4.2%), $MnCl_2$ (8 mM), or **Mn1** (4 mM) in $NaHCO_3$ 4.2%. **a**: Weight variation. **b**: Area under weight curves, * $p < 0.05$ versus control. **c**: Macroscopic scores (mucosal damage, consistency of feces, and mortality). **d**: Colon length. The values are expressed as the mean +/-SEM.

DISCUSSION

To consider the question of the use of SOD mimics *in vivo*, it is important first to characterize them in cells, and to address questions with regard to their stability, speciation, distribution, as well as bio-activity. Herein, we evaluated, in an inorganic biological chemistry approach, the ability of a manganese complex known for its SOD-like activity (**Mn1**),[89, 90] to control inflammatory response in HT29-MD2 intestinal epithelial cells. This work is in line with our previous studies about the development of SODm inspired from Mn-SOD active site towards an optimization of the SOD-like activity[23, 43, 46, 90, 98] and evaluation of anti-oxidant activity in cells.[89]

Biological media abound with coordinating bio-molecules in competition with **L** for Mn^{II}-coordination. Consequently, the question of the speciation of the Mn ion in cells is crucial. The association constants for Mn^{II} are known to be in a weak range for any ligand. This is due to Mn^{II} d^5 electronic state, with 5 electrons in the d-orbitals and no ligand-field stabilization energy. Hence, the criteria for Mn^{II}-complexes stability is far less drastic than with most transition metal ions. The dissociation constant of ligand **L** for Mn^{II} was found to be $0.76 \pm 0.12\ 10^{-6}$ M at pH 7.4. SODm **Mn1** should therefore be stable in presence of biological competitive ligands, such as Human Serum Albumin (HSA) or amino acids,[46] which endow higher dissociation constants for Mn^{II} ($1.2\ 10^{-4}$ M for HSA).[103] The stability of

Mn1 in the growth medium was checked using UV-visible spectroscopy and cyclic voltammetry. The UV-vis and CV signatures of **Mn1** are unchanged over a seven-hour incubation at 37°C in both DMEM and completed growth medium (see Fig. 1), confirming the stability of **Mn1**. In addition, even if Mn^{II} is known to be rather labile,[104, 105] lysate of cells incubated with **Mn1** showed its specific MS-MS signature, indicating that **Mn1** remains at least partially intact in cells (Fig. S3). Moreover, the effect observed on HE conversion attested the anti-superoxide activity of **Mn1** in cells. This experiment is consistent with an intracellular antisuperoxide activity of **Mn1**, as previously shown in the case of macrophages.[89] These results are clear indications that **Mn1** is stable in the experimental conditions of incubation and present in cells, at least for the time-course of the experiments.

The SODm **Mn1** accumulates in HT29-MD2 cells in a time-dependent manner with a maximum concentration reached after about 3h (see Fig. 2). The difference in the intracellular concentration upon incubation with **Mn1** and $MnCl_2$ was qualitatively confirmed by the mappings using X-fluorescence above the K-edge of Mn at the single cell level (see Fig. 3). Synchrotron-based X-ray fluorescence microscopy (μ-SXRF) is a technique giving access to the distribution of heavy elements at the single cell-level without the need of labels and that can be performed on whole cells.[106, 107] Very few examples of subcellular imaging of Mn-SODm have been published.[108] μ-SXRF was performed on cryofixed freeze-dried cells, a procedure that ensures the preservation of the cellular ultrastructure and avoids any artifactual redistribution of diffusible low-molecular weight molecules and ions.[106]

The HT29-MD2 cell line is of interest to evaluate the anti-inflammatory and anti-oxidant activity of **Mn1** in cells as it shows a high sensitivity to LPS, with generation of high levels of inflammatory markers.[93] LPS-induced inflammation is known to be associated with oxidative stress,[8, 13, 14, 91, 92] with overproduction of superoxide in the mitochondria.[8, 91, 92] This is in line with the observation reported here that LPS induces overexpression of active MnSOD.[8, 91] Upon incubation with LPS and **Mn1**, a significant decrease in the MnSOD expression was recorded. No effect of the Zn^{II} redox-inactive analogue **Zn1**, $MnCl_2$ or bovine CuSOD was observed (Fig. 4, S6). The absence of effect of **Zn1**, the Zn^{II} redox-inactive analogue of **Mn1**, is a clear evidence that the activity is associated with the redox Mn-based properties. $MnCl_2$ is shown here to efficiently penetrate inside the HT29-MD2 cells but to be biologically inactive. This supports an activity of the Mn-complex and not of the Mn cation, known to react with superoxide but only slowly and in a non-catalytic manner. Upon incubation with bovine CuSOD, active for the catalysis of the superoxide dismutation but unable to cross cell-membranes,[109] no effect was recorded, highlighting that to be efficient on the inflammation cascade the SOD-activity must be exerted inside cells.

Altogether, these observations on MnSOD expression are of interest as it suggests that SODm **Mn1** efficiently complements the mitochondrial MnSOD, which is consistent with an anti-superoxide intracellular effect of **Mn1**. A similar favorable effect of **Mn1** was recorded on LPS-induced IL8 and COX2 expression, with no effect of **Zn1**, $MnCl_2$, or bovine CuSOD (Fig. 5, S11)

Very interestingly, **Mn1** was shown to be more efficient against inflammation than 5-ASA which is currently used as the first therapeutic line in IBD[11] (see Fig. S7).

For further confirmation of the anti-inflammatory properties of SODm **Mn1**, we performed a preliminary *in vivo* assay using a chemically induced colitis. SODm **Mn1** was orally gavaged in a carbonate buffer to reduce the instability caused by the passage through the acidic medium of the gastro-intestinal tract. Although SODm **Mn1** was probably not in the optimal conditions, a limited but significant effect was recorded on inflammation and health status of the mice. This constitutes an additional evidence that the ability of this complex to accelerate the superoxide dismutation into H_2O_2 is a valuable asset in strategies against inflammatory pathologies.

Conclusion

Antioxidant strategies have been suggested as appropriate to manage IBD.[8, 13, 14, 17, 18] Some other SOD mimics, but few, have been previously shown promising in IBD context.[15] The SOD mimic **Mn1** is an interesting derivative: indeed, it shows an anti-superoxide activity previously characterized out of any cellular context,[90] and in cells.[89] In addition, **Mn1** is easy to synthesize and easily modified, as recently shown.[98] Overall, the approach presented here combining investigation the penetration, speciation and location, with that of the bio-activity, clearly indicates that the SOD mimic **Mn1** is an efficient intracellular anti-inflammatory agent. One important finding of this study is the effect of **Mn1** on mitochondrial MnSOD: **Mn1** is able to complement MnSOD, which has been described as deficient in IBD.[12] In addition, **Mn1** shows a better activity than 5-ASA, already at use in the treatments of IBD, and the oral administration of **Mn1** to *in vivo* model of IBD have led to encouraging results. This is very promising and suggests that the use of this anti-superoxide Mn^{II}-complex as an anti-inflammatory agent could constitute a relevant strategy in the treatment of IBD in particular and more generally of oxidative stress induced diseases.

ASSOCIATED CONTENT

Supporting Information. Chemicals, ITC experiment and **Zn1** CV (Fig S1), EPR spectra (Fig S2); intracellular stability: LC-MS-MS experiment (Fig S3); mapping of P, K, Mn and S in cell (Fig. S4); HE-assay (Fig. S5); complementary control assays (Fig S6, S11), anti-inflammatory activity of 5-ASA (Fig. S10), complementary control assays (Fig S6, S8) and pictures of full blots (Fig. S7-S9); supplementary experimental procedures.

AUTHOR INFORMATION

Corresponding Author

Prof. Clotilde Policar*, Département de Chimie, Ecole Normale Supérieure, PSL Research University — Sorbonne Uni-

versités, UPMC Univ Paris 06, Laboratoire des Biomolecules (LBM), 24, rue Lhomond, 75005 Paris, France E-mail: clotilde.policar@ens.fr

Author Contributions

All authors have given approval to the final version of the manuscript. ‡These authors contributed equally.

Funding Sources

Use of the Advanced Photon Source, an Office of Science User Facility operated for the U.S. Department of Energy (DOE) Office of Science by Argonne National Laboratory, was supported by the U.S. DOE under Contract No. DE-AC02-06CH11357. ENS, CNRS (UMR7203), Université Pierre et Marie Curie Paris 6, ANR (METABACT, TAKE CARE, MAGIC-ANR-15-CE07-0027 projects), *Fondation pour la Recherche Médicale, PSL-Inocellchem*, are acknowledged for financial support. ENS is gratefully acknowledged for A.S.B.'s fellowship and ENS-Cachan for E.M.'s fellowship.

Philippe Seksik declares consulting fees from Abbvie, Merck-MSD and Biocodex, grants from Biocodex, sponsored travel from Merck-MSD and Takeda.

ACKNOWLEDGMENT

We thank TGE RENARD (FR 3443, CNRS) and UMR8601 for access to the EPR spectrometer for the EPR experiments and Dr. Boucher for useful discussions, Institut Curie (Orsay) for free access to cryofixation and freeze-drying facilities and Dr. Guerquin-Kern and Dr. Marco for useful discussions and help in cryofixed samples sample preparation, Dr. Grimaud for access to potentiostat, and APS committee for beamtime. Use of the Advanced Photon Source, an Office of Science User Facility operated for the U.S. Department of Energy (DOE) Office of Science by Argonne National Laboratory, was supported by the U.S. DOE under Contract No. DE-AC02-06CH11357.

Abbreviations

5-ASA: 5-aminosalicylic acid, BSA: bovine serum albumin, COX2: cyclooxygenase 2, DMEM: Dulbecco Modified Eagle Medium, ECL: enhanced chemiluminescence, EDTA: ethylenediaminetetraacetic acid, ELISA: enzyme-linked immunosorbent assay, EPR: electron paramagnetic resonance, HSA: human serum albumin, IBD: inflammatory bowel diseases, IL8: Interleukine 8, ITC: isothermal titration calorimetry, LC: liquid chromatography LDH: lactate dehydrogenase, LPS: lipopolysaccharide, MS: mass spectrometry, NADH: Nicotinamide adenine dinucleotide, NBT: nitro blue tetrazolium, PBS: phosphate buffer saline, ROS: reactive oxygen species, SOD: superoxide dismutase, SXRF: Synchrotron-based X-ray fluorescence microscopy, TEMED: tetramethylethylenediamine

REFERENCES

1. Gilston, B. A.; O'Halloran, T., Mechanisms controlling the metal economy. In *Metals in cells*, Culotta, V.; Scott, R. A., Eds. Wiley: United Kingdom, 2013.
2. Dam, C. S.; Perez Henarejos, S. A.; Tsolakou, T.; Segato, C. A.; Gammelgaard, B.; Yellol, G. S.; Ruiz, J.; Lambert, I. H.; Stürup, S., In vitro characterization of a novel C,N-cyclometalated benzimidazole Ru(II) arene complex: stability, intracellular distribution and binding, effects on organic osmolyte homeostasis and induction of apoptosis. *Metallomics* **2015,** *7*, 885-895.
3. Gasser, G., *Inorganic Chemical Biology — Principles, Techniques and Applications*. Wiley: United Kingdom, 2014.
4. Clède, S.; Lambert, F.; Saint-Fort, R.; Plamont, M. A.; Bertrand, H.; Vessières, A.; Policar, C., *Chem. Eur. J.* **2014,** *20*, 8714-8722.
5. Clède, S.; Lambert, F.; Saint-Fort, R.; Plamont, M. A.; Bertrand, H.; Vessières, A.; Policar, C., Influence of the Side-Chain Length on the Cellular Uptake and the Cytotoxicity of Rhenium Triscarbonyl Derivatives: A Bimodal Infrared and Luminescence Quantitative Study. *Chem. Eur. J.* **2014,** *20*, 8714-8722.
6. We wish thank one of the referee who underlined the importance of the approach and for encouraging us to stress this idea.
7. Halliwell, B.; Gutteridge, J. M. C., *Free radicals in biology and medicine*. Oxford University Press: New York, 2007.
8. Valentine, J. F.; Nick, H. S., Acute-phase induction of manganese superoxide dismutase in intestinal epithelial cell lines. *Gastroenterology* **1992,** *103*, 905-912.
9. Biasi, F.; Leonarduzzi, G.; Oteiza, P. I.; Poli, G., Inflammatory Bowel Disease: Mechanisms, Redox Considerations, and Therapeutic Targets. *Antiox. Redox Signal.* **2013,** *19*, 1711-1747.
10. Zhu, H.; Li, Y. R., Oxidative stress and redox signaling mechanisms of inflammatory bowel disease: upsated experimental and clinical evidence. *Exp. Biol. Med.* **2012,** *237*, 474-480.
11. Rezaie, A.; Parker, R. D.; Abdollahi, M., Oxidative stress and pathogenesis of inflammatory bowel disease: An epiphenomenon or the cause? *Dig. Dis. Sci.* **2007,** *52*, 2015-2021.
12. Kruidenier, L.; Kuiper, I.; van Duijn, W.; Marklund, S. L.; van Hogezand, R. A.; Lamers, C. B. H. W.; Verspaget, H. W., Differential mucosal expression of three SOD isoforms in inflammatory bowel disease. *J. Pathol.* **2003,** *201*, 7-16.
13. Denis, M. C.; Furtos, A.; Dieudonné, S.; Montoudis, A.; Garofalo, C.; Desjardins, Y.; Delsvin, E.; Levy, E., Apple Peel Polyphenols and Their Beneficial Actions on Oxidative Stress and Inflammation. *PLoS One* **2013,** *8*, e53725.
14. Russo, I.; Luciani, A.; De Cicco, P.; Troncone, E.; Ciacci, C., Butyrate Attenuates Lipopolysaccharide-Induced Inflammation in Intestinal Cells and Crohn's Mucosa through Modulation of Antioxidant Defense Machinery. *Plos one* **2012,** *7*, e32841.
15. Cuzzocrea, S.; Mazzon, E.; Dugo, L.; Caputi, A. P.; Riley, D. P.; Salvemini, D., Protective effects of M40403 a superoxide dismutase mimetic in a rodent model of colitis. *Eur. J. Pharmacol* **2001,** *432*, 79-89.
16. Wang, Y.-H.; Dong, J.; Zhang, J.-X.; Zhai, J.; Ge, B., Effects of mimic of manganese superoxide dismutase on 2,4,6-trinitrobenzene sulfonic acid-induced colitis in rats. *Arch. Pharm. Res.* **2016,** *39*, 1296-1307.
17. Simmonds, N. J.; Millar, A. D.; Blake, D. R.; Rampton, D. S., Antioxidant effects of aminosalicylates and potential new drugs for inflammatory bowel disease: assessment in cell-free systems and in inflamed human colorectal biopsies. *Aliment. Pharm. Ther.* **1999**, 363-372.
18. Millar, A. D.; Rampton, D. S.; Chander, A. W. D.; Blades, S.; Coumbe, A.; Panetta, J.; Morris, C. J.; Blake, D. R., Evaluating the antioxidant potential of new treatments for inflammatory bowel disease using a rat model of colitis. *Gut* **1996,** *39*, 407-415.
19. Segui, J.; Gironella, M.; Sans, M.; Granell, S.; Gil, F.; Gimeno, M.; Coronel, P.; Pique, J. M.; Panes, J., Superoxide dismutase ameliorates TNBS-induced colitis by reducing oxidative stress, adhesion molecule expression, and leukocyte recruitment into the inflamed intestine. *J. Leukoc. Biol.* **2004,** *76*, 537-544.

20. Salvemini, D.; Muscoli, C.; Riley, D. P.; Cuzzocrea, S., Superoxide dismutases mimetics. *Pulm. Pharmacol. Ther.* **2002,** *15*, 439-447.
21. Iranzo, O., Manganese complexes displaying superoxide dismutase activity: A balance between different factors. *Bioorg. Chem.* **2011,** *39*, 73-87.
22. Batinic-Haberle, I.; Tovmasyan, A.; Roberts, E. R.; Vujaskovic, Z.; Leong, K. W.; Spasojevic, I., SOD Therapeutics: Latest Insight into Their Structure-Activity Relationships and Impact on the Cellular Redox-based Signaling Pathways. *Antioxid Redox Signal.* **2014,** *20*, 2372-2415.
23. Policar, C., Mimicking SODs, Why and How: Bio-Inspired Manganese Complexes as SOD Mimics. In *Redox Active Therapeutics*, Reboucas, J. S.; Batinic-Haberle, I.; Spasojevic, I.; Warner, D. S.; St. Clair, D., Eds. Springer: 2016; pp 125-164.
24. Batinic-Haberle, I.; Reboucas Julio, S.; Spasojevic, I., SOD mimic: chemistry, pharmacology and therapeutic potential. *Antioxid Redox Signal.* **2010,** *13*, 877-918.
25. Miriyala, S.; Spasojevic, I.; Tovmasyan, A.; Salvemini, D.; Vujaskovic, Z.; St. Clair, D.; Batinic-Haberle, I., MnSOD and its mimics. *Biochim. Biophys. Acta* **2012**, 794-814.
26. Charrier, J. G.; Anastasio, C., Impacts of antioxidants on hydroxyl radical production from individual and mixed transition metals in a surrogate lung fluid. *Atmos. Environ.* **2011,** *45*, 7555-7562.
27. Tovmasyan, A.; Carballal, S.; Ghazaryan, R.; Melikyan, L.; Weitner, T.; Maia, C. G. C.; Reboucas, J. S.; Radi, R.; Spasojevic, I.; Benov, L.; Batinic-Haberle, I., Rational Design of Superoxide Dismutase (SOD) Mimics: The Evaluation of the Therapeutic Potential of New Cationic Mn Porphyrins with Linear and Cyclic Substituents. *Inorg. Chem.* **2014,** *53*, 11467-11483.
28. Archibald, F. S.; Fridovich, I., Mn and defenses against oxygen toxicity in Lactobacillus plantarum. *J. Bacteriol.* **1981,** *445*, 442-451.
29. Barnese, K.; Gralla, E. B.; Cabelli, D. E.; Valentine, J. S., Manganous phosphate acts as a SOD. *J. Am. Chem. Soc.* **2008,** *130*, 4604-4606.
30. Baudry, M.; Etienne, S.; Bruce, A.; Palucki, M.; Jacobsen, E.; Malfroy, B., Salen-manganese complexes are superoxide dismutase-mimics. *Biochem. Biophys. Res. Commun.* **1993,** *192*, 964-968.
31. Puglisi, A.; Tabb, G.; Vecchio, G., Bioconjugates of cyclodextrins of manganese salen-type with superoxide dismutase activity. *J. Inorg. Biochem.* **2004,** *98*, 969–976.
32. Park, W.; Lim, D., Effect of oligo(ethyleneglycol) group on the antioxidant activity of manganese-salen complexes. *Biorganic and medicinal chemistry letters* **2009,** *19*, 614-617.
33. Rush, J. D.; Maskos, Z.; Koppenol, W. H., The SOD activities of two higher valent Mn(IV) desferrioxamine and Mn(III)cyclam. *Arch. Biochem. Biophys.* **1991,** *289*, 97-102.
34. Riley, D. P.; Weiss, R. H., Manganese macrocyclic ligand complexes as mimics for SOD. *J. Am. Chem. Soc.* **1994,** *116*, 387-388.
35. Riley, D. P.; Henke, S. L.; Lennon, P. J.; Weiss, R. H.; Neumann, W. L.; Rivers, W. J. J.; Aston, K. W.; Sample, K. R.; Rahman, H.; Ling, C.-S.; Shieh, J.-J.; Busch, D. H.; Szulbinski, W., Synthesis characterization and stability of Mn(II) complexes. *Inorg. Chem.* **1996,** *119*, 5213-5231.
36. Riley, D. P.; Henke, S. L.; Lennon, P. J.; Aston, K., Computer-Aided Design (CAD) of synzymes : use of MM for rational design of SOD mimics. *Inorg. Chem.* **1999,** *38*, 1908-1917.
37. Salvemini, D.; Wang, Z.-Q.; Zweier, J. L.; Samouilov, A.; Macarthur, H.; Misko, T. P.; Currie, M. G.; Cuzzocrea, S.; Sikorski, J. A.; Riley, D. P., A non-peptidyl mimic of SOD with therapeutic activity in rats. *Science* **1999,** *286*, 304-305.
38. Dees, A.; Zahl, A.; Puchta, R.; van Eikema Hommes, N. J. R.; Heinemann, F. W.; Ivanovic-Burmazovic, I., Water exchange on seven-coordinate Mn(II) complexes with macrocyclic pentadentate ligands: insight in the mechanism of Mn(II) SOD-mimetic. *Inorg. Chem.* **2007,** *46*, 2459-2470.
39. Kitajima, N.; Osawa, M.; Tamura, N.; Moro-Oka, Y.; Hirano, T.; Hirobe, M.; Nagano, T., Monomeric (benzoato)manganese(II) complexes as manganese superoxide dismutase mimics. *Inorg. Chem.* **1993,** *32*, 1879-1880.
40. Deroche, A.; Morgenstern-Badarau, I.; Cesario, M.; Guilhem, J.; Keita, B.; Nadjo, L.; Houée-Levin, C., A seven coordinate Mn(II) complex formed with a single tripodal heptadentate ligand as a new superoxide scavenger. *J. Am. Chem. Soc.* **1996,** *118*, 4567-4573.
41. Xiang, D. F.; Tan, X. S.; Hang, Q. W.; Tang, W. X.; Wu, B.-M.; Mak, T. C. W., Crystal structure and properties of a new five-coordinate manganese superoxide dismutase mimic. *Inorg. Chim. Acta* **1998,** *277*, 21–25.
42. Yamato, K.; Miyahara, I.; Ichimura, A.; Hirotsu, K.; Kojima, Y.; Sakurai, H.; Shiomi, D.; Sato, K.; Takui, T., Superoxide dismutase mimetic complex of Mn(II) / N,N-bis(2-pyridylmethyl)-(S)-histidine. *Chem. Lett.* **1999**, 295-296.
43. Policar, C.; Durot, S.; Lambert, F.; Cesario, M.; Ramiandrasoa, F.; Morgenstern-Badarau, I., New Mn(II) complexes with N/O coordination sphere from tripodal N-centered ligands. Characterization from solid state to solution and reaction with superoxide in non-aqueous and aqueous medium. *Eur. J. Inorg. Chem.* **2001**, 1807-1818.
44. Lewis, E. A.; Khodr, H. H.; Hider, R. C.; Lindsay-Smith, J. R.; Walton, P. H., A manganese superoxide dismutase mimic based on cis-cis-1,3,5-triaminocyclohexane. *J. Chem. Soc., Dalton trans* **2004**, 187-188.
45. Durot, S.; Lambert, F.; Renault, J.-P.; Policar, C., A pulse radiolysis study of superoxide radical catalytic dismutation by a manganese(II) complex with a N-tripodal ligand. *Eur. J. Inorg. Chem.* **2005**, 2789-2793.
46. Durot, S.; Policar, C.; Cisnetti, F.; Lambert, F.; Renault, J.-P.; Pelosi, G.; Blain, G.; Korri-Youssoufi, H.; Mahy, J.-P., Series of Mn Complexes Based on N-Centered Ligands and Superoxide – Reactivity in an Anhydrous Medium and SOD-Like Activity in an Aqueous Medium Correlated to MnII/MnIII Redox Potentials. *Eur. J. Inorg. Chem.* **2005**, 3513-3523.
47. Liao, Z.-R.; Zheng, X.-F.; Luo, B.-S.; Shen, L.-R.; Li, D.-F.; Liu, H.-L.; Zhao, W., Synthesis, characterization and SOD-like activities of manganese-containing complexes with N,N,N',N'-tetrakis(2'-benzimidazolyl methyl)-1,2-ethanediamine (EDTB). *Polyhedron* **2001,** *20*, 2813-2821.
48. Groni, S.; Blain, G.; Guillot, R.; Policar, C.; Anxolabéhère-Mallart, E., Reactivity of Mn(II) with superoxide. Evidence for a [Mn(III)OO]+ unit by low-Temperature spectroscopies. *Inorg. Chem.* **2007,** *46*, 1951-1953.
49. Cisnetti, F.; Pelosi, G.; Policar, C., Synthesis and superoxide dismutase-like activity of new manganese(III) complexes based on tridentate N2O ligands derived from histamine. *Inorg. Chim. Acta* **2007,** *360*, 557-562.
50. Beyer, W. F.; Fridovich, I., Characterization of a SOD mimic prepared from desferrioxamine and MnO2. *Arch. Biochem. Biophys.* **1989,** *271*, 149-156.
51. Faulkner, K. M.; Stevens, R. D.; Fridovich, I., Characterization of Mn(III) complexes of linear and cyclic desferrioxamines as mimics of SOD activity. *Arch. Biochem. Biophys.* **1994,** *310*, 341-346.
52. Lati, J.; Meyerstein, D., Oxidation of the first-row divalent transition metal complexes containing ethylendiaminetetraacetate and nitrilotriacetate ligands by free radicals : a pulse radiolyse study. *J. Chem. Soc., Dalton Trans.* **1978**, 1105-1118.

53. Stein, J.; Fackler, J. P.; McClune, G. J.; Fee, J. A.; Chan, L. T., Superoxide and Manganese(III). Reaction of Mn-EDTA and Mn-CyDTA complexes with (O2)-. Xray structure of KMnEDTA.2H2O. *Inorg. Chem.* **1979,** *18*, 3511-3518.
54. Koppenol, W. H.; Levine, F.; Hatmaker, T. L.; Epp, J.; Rush, J. D., Catalysis of superoxide dismutation by Mn-aminopolycarboxylate complexes. *Arch. Biochem. Biophys.* **1986,** *251*, 594-599.
55. Archibald, F. S.; Fridovich, I., The scavenging of superoxide radical by manganous complexes: in vitro. *Arch. Biochem. Biophys.* **1982,** *214*, 452-463.
56. Bailey, M. A.; Ingram, M. J.; Naughton, D. P., A novel antioxidant and anti-cancer strategy: a peptoid antiinflammatory drug conjugate with SOD mimic activity. *Biochem. Biophys. Res. Commun.* **2004,** *317*, 1155-1158.
57. Fisher, A. E. O.; Naughton, D. P., Metal ion chelating peptides with superoxide dismutase activity. *Biomedicine & Pharmacotherapy* **2005,** *59*, 158–162.
58. Piacham, T.; Isarankura-Na-Ayudhya, C.; Nantasenamat, C.; Yainoy, S.; Ye, L.; Bülow, L.; Prachayasittihul, N., Metalloantibiotic Mn(II)-bacitracin complex mimicking manganese superoxide dismutase. *Biochem. Biophys. Res. Commun.* **2006,** *341*, 925-930.
59. Valentine, J. S.; Quinn, A. E., Reaction of superoxide with Mn(III)tetraphenylporphyrin cation. *Inorg. Chem.* **1976,** *15*, 1997-1999.
60. Faulkner, K. M.; Liochev, S. I.; Fridovich, I., Stable Mn(III) porphyrins mimic SOD in vitro and substitute for it in vivo. *J. Biol. Chem.* **1994,** *269*, 23471-23476.
61. Batinic-Haberle, I.; Liochev, S. I.; Spasojevic, I.; Fridovich, I., A potent SOD mimic: Mnßoctabromo meso-tetrakis(N-methylpyridinium-4-yl)porphyrin. *Arch. Biochem. Biophys.* **1997,** *343*, 225-233.
62. Batinic-Haberle, I.; Benov, L.; Spasojevic, I.; Fridovich, I., The ortho effect makes Mn(III)porphyrins a powerfull potentially used SOD mimic. *J. Biol. Chem.* **1998,** *273*, 24521-24528.
63. Gauuan, P. J. F.; Trova, M. P.; Gregor-Boros, L.; Bocckino, S. B.; Crapo, J. D.; Day, B. J., Superoxide Dismutase Mimetics: Synthesis and Structure–Activity Relationship Study of MnTBAP Analogues. *Bio. Med. Chem* **2002,** *10*, 3013-3021.
64. Batinic-Haberle, I.; Spasojevic, I.; Stevens, R. D.; Bondurant, B.; Okado-Matsumoto, A.; Fridovich, I.; Vujaskovic, Z.; Dewhirsta, M. W., New PEG-ylated Mn(III) porphyrins approaching catalytic activity of SOD enzyme. *Dalton Trans* **2006**, 617-624.
65. Matemadombo, F.; Durmus, M.; Escriou, V.; Griveau, S.; Scherman, D.; Bedioui, F.; Nyokong, T., Evaluation of the performance of manganese phthalocyanines as superoxide dismutase mimics. *Curr. Anal. Chem.* **2009,** *5*, 330-338.
66. Spasojevic, I.; Batinic-Haberle, I.; Stevens, R. D.; Hambright, P.; Thorpe, A. N.; Grodkowski, J.; Neta, P.; Fridovich, I., Mn(III) biliverdin IX dimethylester: a powerful catalytic scavenger of superoxide employing the Mn(III)/Mn(IV) redox couple. *Inorg. Chem.* **2001,** *40*, 726-739.
67. Gauter-Fleckenstein, B.; Fleckenstein, K.; Owzar, K.; Jiang, C.; Batinic-Haberle, I.; Vujaskovic, Z., Comparison of two Mn porphyrin-based mimics of superoxide dismutase in pulmonary radioprotection. *Free Radical Biol. Med.* **2008,** *44*, 982-9.
68. Gauter-Fleckenstein, B.; Fleckenstein, K.; Owzar, K.; Jiang, C.; Reboucas, J. S.; Batinic-Haberle, I.; Vujaskovic, Z., Early and late administration of MnTE-2-PyP5+ in mitigation and treatment of radiation-induced lung damage. *Free Radical Biol. Med.* **2010,** *48*, 1034-1043.
69. Pearlstein, R. D.; Higuchi, Y.; Moldovan, M.; Johnson, K.; Fukuda, S.; Gridley, D. S.; Crapo, J. D.; Warner, D. S.; Slater, J. M., Metalloporphyrin antioxidants ameliorate normal tissue radiation damage in rat brain. *Int. J. Radiat. Biol.* **2010,** *86*, 145-163.
70. Doctrow, S. R.; Lopez, A.; Schock, A. M.; Duncan, N. E.; Jourdan, M. M.; Olasz, E. B.; Moulder, J. E.; Fish, B. L.; Mader, M.; Lazar, J.; Lazarova, Z., A Synthetic Superoxide Dismutase/Catalase Mimetic EUK-207 Mitigates Radiation Dermatitis and Promotes Wound Healing in Irradiated Rat Skin. *Journal of Investigative Dermatology* **2013,** *133*, 1088-1096.
71. Alexandre, J.; Nicco, C.; Chereau, C.; Laurent, A.; Weill, B.; Goldwasser, F.; Batteux, F., Improvement of the therapeutic index of anticancer drugs by the superoxide dismutase mimic mangafodipir. *J. Natl. Cancer Inst.* **2006,** *98*, 236-44.
72. Bedda, S.; Laurent, A.; Conti, F.; Chereau, C.; Tran, A.; Tran-Van Nhieu, J.; Jaffray, P.; Soubrane, O.; Goulvestre, C.; Calmus, Y.; Weill, B.; Batteux, F., Mangafodipir prevents liver injury induced by acetaminophen in the mouse. *J. Hepatol.* **2003,** *39*, 765-72.
73. Doctrow, S. R.; Huffman, K.; Marcus, C. B.; Tocco, G.; Malfroy, E.; Adinolfi, C. A.; Kruk, H.; Baker, K.; Lazarowych, N.; Mascarenhas, J.; Malfroy, B., Salen-Mn as catalytic scavengers of H202 and cytoprotective agents: SAR studies. *J. Med. Chem.* **2002,** *45*, 4549-4558.
74. Sheng, H.; Enghild, J. J.; Bowler, R.; Patel, M.; Batinic-Haberle, I.; Calvi, C. L.; Day, B. J.; Pearlstein, R. D.; Crapo, J. D.; Warner, D. S., Effects of metalloporphyrin catalytic antioxidants in experimental brain ischemia. *Free Radical Biol. Med.* **2002,** *33*, 947-961.
75. Brurok, H.; Ardenkjaer-Larsen, J. H.; Hansson, G.; Skarra, S.; Berg, K.; Karlsson, J. O. G.; Laursen, I.; Jynge, P., Manganese dipyridoxyl diphosphate: MRI contrast agent with antioxidative and cardioprotective properties? . *Biochem. Biophys. Res. Commun.* **1999,** *254*, 768-772.
76. Masini, E.; Cuzzocrea, S.; Mazzon, E.; Marzocca, C.; Mannaioni, P. F.; Salvemini, D., Protective effect of M40403, a selective SOD mimetic in myocardial and reperfusion injury *in vivo*. *Br. J. Pharmacology* **2002,** *136*, 905-917.
77. Rong, Y.; Doctrow, S. R.; Tocco, G.; Baudry, M., EUK-134, a synthetic SOD and catalase mimetic prevents oxidative stress and attenuate kainate-induced neuropathology. *Proc. Natl. Acad. Sci. USA* **1999,** *96*, 9897-9902.
78. Vajragupta, O.; Boonchoong, P.; Sumanot, Y.; Watanabe, Y.; Wongkrajang, Y.; Kammasud, N., Mn-based complexes of radical scavengers as neuroprotective agents. *Bio. Med. Chem* **2003,** *11*, 2329-2337.
79. McDonald, M. C.; d'Emmanuele di Villa Bianca, R.; Wayman, N. S.; Pinto, A.; Sharpe, M. A.; Cuzzocrea, S.; Chatterjee, P. K.; Thiemermann, C., A SOD mimetic with catalase activity (EUK-8) reduces the organ injury in endotoxic shock. *Eur. J. Pharmacol.* **2003,** *466*, 181-189.
80. Batinic-Haberle, I.; Benov, L. T., An SOD mimic protects NADP+-dependent isocitrate dehydrogenase against oxidative inactivation. *Free Radical Res.* **2008,** *42*, 618-624.
81. Masini, E.; DBani, D.; Vannacci, A.; Pierpaoli, S.; Mannaioni, P. F.; Comhair, S. A. A.; Xu, W.; Muscoli, C.; Erzurum, S. C.; Salvemini, D., Reduction of antigen-induced respiratory abnormalities and airway inflammation in sensitized guinea pigs by a SOD mimetic. *Free Radical Biol. Med.* **2005,** *39*, 520-531.
82. Patel, M. N., Metalloporphyrines improve the survival of SOD2 deficient neurons. *Aging Cell* **2003,** *2*, 219-222.
83. Okado-Matsumoto, A.; Batinic-Haberle, I.; Fridovich, I., Complementation of SOD-deficient Escherichia coli by manganese porphyrin mimics of superoxide dismutase activity. *Free Radical Biol. Med.* **2004,** *37*, 401-410.
84. Munroe, W.; Kingsley, C.; Durazo, A.; Butler Gralla, E.; Imlay, J. A.; Srinivasan, C.; Valentine, J. S., Only one of a

wide assortment of manganese-containing SOD mimicking compounds rescues the slow aerobic growth phenotypes of both Escherichia coli and Saccharomyces cerevisiae strains lacking superoxide dismutase enzymes. *J. Inorg. Biochem.* **2007,** *101* 1875–1882.
85. Moeller, B. J.; Batinic-Haberle, I.; Spasojevic, I.; Rabbani, Z. N.; Anscher, M. S.; Vujaskovic, Z.; Dewhirst, M. W., A manganese porphyrin superoxide dismutase mimetic enhances tumor radioresponsiveness. *Int. J. Radiat. Oncol., Biol., Phys.* **2005,** *63*, 545-552.
86. Pollard, J. M.; Reboucas, J. S.; Durazo, A.; Kos, I.; Fike, F.; Panni, M.; Butler Gralla, E.; Valentine, J. S.; Batinic-Haberle, I.; Gatti, R. A., Radioprotective effects of manganese-containing superoxide dismutase mimics on ataxia-telangiectasia cells. *Free Radical Biol. Med.* **2009,** *47*, 250-60.
87. Vorotnikova, E.; Rosenthal, R. A.; Tries, M.; Doctrow, S. R.; Braunhuta, S. J., Novel Synthetic SOD/Catalase Mimetics Can Mitigate Capillary Endothelial Cell Apoptosis Caused by Ionizing Radiation. *Radiation Research* **2010,** *173*, 748–759.
88. Filipovic, M. R.; Koh, A. C. W.; Arbault, S.; Niketic, V.; Debus, A.; Schleicher, U.; Bogdan, C.; Guille, M.; Lemaitre, F.; Amatore, C.; Ivanovic-Burmazovic, I., Striking inflammation from both sides: manganese(II)pentaazamacrocyclic SOD mimics act also as nitric oxide dismutases: a single-cell study. *Angew. Chem., Int. ed. Engl.* **2010,** *49*, 4228-4232.
89. Bernard, A.-S.; Giroud, C.; Ching, H. Y. V.; Meunier, A.; Ambike, V.; Amatore, C.; Guille Collignon, M.; Lemaître, F.; Policar, C., Evaluation of the Anti-Oxidant Properties of a SOD-mimic Mn-Complex in Activated Macrophages. *Dalton Trans.* **2012,** *41*, 6399-6403.
90. Cisnetti, F.; Lefevre, A. S.; Guillot, R.; Lambert, F.; Blain, G.; Anxolabéhère-Mallart, E.; Policar, C., A new pentadentate ligands forms both a di- and mononuclear Mn(II) complex: electrochemical, spectrosocpic and SOD activity studies. *Eur. J. Inorg. Chem.* **2007**, 4472-4480.
91. Nick, H. S.; Rogers, R. J.; Monnier, J. M., Tumor Necrosis Factor-a Selectively Induces MnSOD Expression via Mitochondria-to-Nucleus Signaling, whereas Interleukin-1ß Utilizes an Alternative Pathway. *J. Biol. Chem.* **2001,** *276*, 20419-20427.
92. Chan, S. H. H.; Wub, K. L. H.; Wang, L. L.; Chan, J. Y. H., Nitric oxide- and superoxide-dependent mitochondrial signalling in endotoxin-induced apoptosis in the rostral ventrolateral medulla of rats. *Free Radical Biol. Med.* **2005,** *39*, 603-618.
93. Lenoir, C.; Sapin, C.; Broquet, A. H.; Jouniaux, A.-M.; Bardin, S.; Gasnereau, I.; Thomas, G.; Seksik, P.; Trugnan, G.; Masliah, J.; Bachelet, M., MD-2 controls bacterial lipopolysaccharide hyporesponsiveness in human intestinal epithelial cells. *Life Sci.* **2008,** *82*, 519-528.
94. Seksik, P.; Sokol, H.; Grondin, V.; Adrie, C.; Duboc, H.; Pigneur, B.; Thomas, G.; Beaugerie, L.; Trugnan, G.; Masliah, J.; Bachelet, M., Sera from patients with Crohn's disease break bacterial lipopolysaccharide tolerance of human intestinal epithelial cells via MD-2 activity. *Innate Imunnity* **2010,** *16*, 381-390.
95. Weydert, C. J.; Cullen, J. J., Measurement of superoxide dismutase, catalase and glutathione peroxidase in cultured cells and tissue. *Nature protocols* **2010,** *5*, 51-66.
96. Barrette, W. C. J.; Sawyer, D. T.; Fee, J. A.; Asada, K., Potentiometric titration and oxidation-reduction potentials of several iron superoxide dismutases. *Biochemistry* **1983,** *22*, 624-627.
97. Batinic-Haberle, I.; Spasojevic, I.; Stevens, R. D.; Hambright, P.; Neta, P.; Okado-Matsumoto, A.; Fridovich, I., New class of potent catalysts of superoxide dismutation. Mn(III) ortho-methoxyethylpyridyl- and di-ortho-methoxyethyl-imidazolylporphyrins. *J. Chem. Soc., Dalton trans.* **2004**, 1696-1702.
98. Ching, H. Y. V.; Kenkel, I.; Delsuc, N.; Mathieu, E.; Ivanović-Burmazovic, I.; Policar, C., Bioinspired superoxide-dismutase mimics: the effects of functionalization with cationic polyarginine peptides. *J. Inorg. Biochem.* **2016,** *160*, 172-179.
99. Ash, D. E.; Schramm, V. L., Determination of free and bound manganese(II) in hepatocytes from fed and fasted rats. *J. Biol. Chem.* **1982,** *257*, 9261-9264.
100. Carmona, A.; Devès, G.; Roudeau, S.; Cloetens, P.; Bohic, S.; Ortega, R., Manganese Accumulates within Golgi Apparatus in Dopaminergic Cells as Revealed by Synchrotron X-ray Fluorescence Nanoimaging. *ACS Chemical Neuroscience* **2010,** *1*, 194-203.
101. Robinson, K. M.; Janes, M. S.; Pehar, M.; Monette, J. S.; Ross, M. F.; Hagen, T. M.; Murphy, M. P.; Beckman, J. S., Selective fluorescent imaging of superoxide in vivo using ethidium-based probes. *Proc. Natl. Acad. Sci. U.S.A.* **2006,** *103*, 15038-15043.
102. Lyublinskaya, O. G.; Zenin, V. V.; Shatrova, A. N.; Aksenov, N. D.; Zemelko, V. I.; Domnina, A. P.; Litanyuk, A. P.; Burova, E. B.; Gubarev, S. S.; Negulyaev, Y. A.; Nikolsky, N., N, Intracellular oxidation of hydroethidine: Compartmentalization and cytotoxicity of oxidation product. *Free Rad. Biol. & Med* **2014,** *75*, 60-68.
103. Xingcan, S.; Hong, L.; Zhiliang, J.; Xiwen, H.; Panwen, P., Binding equilibrium study between Mn(II) and HSA or BSA. *Chin. J. Chem.* **2000,** *18*, 35-41.
104. Barnese, K.; Butler Gralla, E.; Valentine, J. S.; Cabelli, D. E., Biologically relevant mechanism for catalytic superoxide removal by simple manganese compounds. *Proc. Natl. Acad. Sci. U.S.A.* **2012,** *109*, 6892-6897.
105. McNaughton, R. L.; Reddi, A. R.; Clement, M. H. S.; Sharma, A.; Barnese, K.; Rosenfeld, L.; Butler Gralla, E.; Valentine, J. S.; Culotta, V. C.; Hoffman, B., Probing in vivo Mn2+ speciation and oxidative stress resistance in yeast cells with electron-nuclear double resonance spectroscopy. *Proc. Natl. Acad. Sci. U.S.A.* **2010,** *107*, 15335-15339.
106. McRae, R.; Bagchi, P.; Sumalekshmy, S.; Fahrni, C. J., In situ imaging of metals in cells and tissues. *Chem. Rev.* **2009,** *109*, 4780-4827.
107. Qin, Z.; Caruso, J. A.; Lai, B.; Matusche, A.; Beckerf, J. S., Trace metal imaging with high spatial resolution: Applications in biomedicine. *Metallomics* **2011,** *3*, 28-37.
108. Aitken, J. B.; Shearer, E. L.; Giles, N. M.; Lai, B.; Vogt, S.; Reboucas, J. S.; Batinic-Haberle, I.; Lay, P. A.; Giles, G. I., Intracellular targeting and pharmacological activity of the SOD mimics MnTE-2-PyP(5+) and MnTnHex-2-PyP(5+) regulated by their porphyrin ring substituents. *Inorg. Chem.* **2013,** *52*, 4121-4123.
109. Abreu, I. A.; Cabelli, D. E., Superoxide dismutases—a review of the metal-associated mechanistic variations. *Biochim. Biophys. Acta* **2010,** *1804*, 263–274.

Table of contents synopsis

A Mn-complex SOD-mimic was studied in intestinal cell line, HT29-MD2, in which oxidative stress and inflammation was induced using bacterial lipopolysaccharide. This complex was shown to enter cells where it exerts an efficient specific anti-inflammatory activity, to be present in cell lysates, and to have a distribution all over the cell, with the ability to functionally complement the mitochondrial MnSOD.

Table of contents graphic

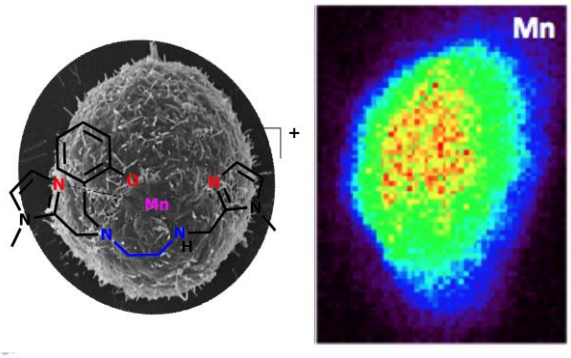

For Table of Contents only